

Aerosol hygroscopicity and CCN activity during the AC³Exp campaign: Implications for CCN parameterization

Fang Zhang¹, Yanan Li¹, Zhanqing Li*^{1,2}, Li Sun³, Runjun Li¹,
Chuanfeng Zhao¹, Pucui Wang³, Yele Sun⁴, Xinggong Liu⁵, Junxia
5 Li^{6,7}, Peiren Li⁶, Gang Ren⁶, Tianyi Fan¹

¹*College of Global Change and Earth System Science, Beijing Normal University, Beijing 100875, China*

²*Earth System Science Interdisciplinary Center and Department of Atmospheric and Oceanic Science, University of Maryland, College Park, Maryland, USA.*

10 ³*Key Laboratory of Middle Atmosphere and Global Environment Observation (LAGEO), Institute of Atmospheric Physics, Chinese Academy of Sciences, Beijing, 100029, China*

⁴*State Key Laboratory of Atmospheric Boundary Layer Physics and Atmospheric Chemistry, Institute of Atmospheric Physics, Chinese Academy of Sciences, Beijing
15 100029, China*

⁵*State Key Laboratory of Water Environment Simulation, School of Environment, Beijing Normal University, Beijing 100875, China*

⁶*Weather Modification Office of Shanxi Province, Taiyuan, China, 030032*

⁷*Key Laboratory for Aerosol-Cloud-Precipitation of China Meteorological Administration, Nanjing University of Information Science and Technology, Nanjing, China, 21
20 0044*

***correspondence to: Z. Li (zli@atmos.umd.edu)**

25

Abstract

Aerosol hygroscopicity and cloud condensation nuclei (CCN) activity under background conditions and during polluted events are investigated during the Aerosol-CCN-Cloud Closure Experiment (AC³Exp) campaign conducted at Xianghe, China in summer 2013. A gradual increase in size-resolved activation ratio (AR) with particle diameter (D_p) suggests that aerosol particles have different hygroscopicities. During pollution events, the activation diameter (D_a) measured at low supersaturation (SS) was significantly increased compared to background conditions. An increase was not observed when SS > 0.4%. The hygroscopicity parameter kappa (κ) was ~0.31-0.38 for particles in accumulation mode under background conditions. This range in magnitude of κ is ~20% higher than κ derived under polluted conditions. For particles in nucleation or Aitken mode, κ ranged from 0.20-0.34 for background and polluted cases. Larger particles were on average more hygroscopic than smaller particles. The situation is more complex for heavy pollution particles because of the diversity in particle composition and mixing state. A non-parallel observation CCN closure test showed that uncertainties in CCN number concentration estimates ranged from 30%-40%, which are associated with changes in particle composition as well as measurement uncertainties associated with bulk and size-resolved CCN methods. A case study showed that bulk CCN activation ratios increased as total condensation nuclei (CN) number concentrations (N_{CN}) increased on background days. The background case also showed that bulk AR correlated well with the hygroscopicity parameter calculated from chemical volume fractions. On the contrary, bulk AR

decreased with increasing total N_{CN} during polluted events, but was closely related to f_{44} , which is usually associated with the particle organic oxidation level. Our study highlights the importance of chemical composition on determining particle activation properties and underlines the significance of long-term observations of CCN under

5 different atmospheric environments, especially regions with heavy pollution.

1. Introduction

The indirect influence of aerosol particles on the radiative balance of the atmosphere through changes in cloud droplet number and the persistence of clouds (Twomey, 1974; Albrecht, 1989) carries the largest uncertainty amongst the presently known causes of radiative forcing (IPCC, 2007, 2013). Thus, better understanding of aerosol particle formation, growth, and activation is essential.

Field and laboratory experiments have been conducted with the aim of better characterizing the particle physical and chemical parameters impacting on cloud condensation nuclei (CCN) activation. Studies have addressed the relative importance of the size distribution, particle composition, and mixing state in determining CCN activation, but there are disagreements on the relative importance of these parameters (e.g., Roberts et al., 2002; Feingold, 2003; Ervens et al., 2005; Mircea et al., 2005; Dusek et al., 2006a; Anttila and Kerminen, 2007; Hudson, 2007; Quinn et al., 2008; Zhang et al., 2008; Deng et al., 2013, Ma et al., 2013). CCN closure studies are a useful approach to test our knowledge of the controlling physical and chemical factors and to help verify experimental results. The CCN number concentration (N_{CCN}) is usually predicted from measured aerosol properties such as particle number size distribution and composition or hygroscopicity based on Köhler theory. The closure between the measured and estimated N_{CCN} is often achieved under background atmospheric conditions without heavy pollution (Chuang et al., 2000; Dusek et al., 2003; VanReken et al., 2003; Rissler et al., 2004; Gasparini et al., 2006; Stroud et al., 2007; Bougiatioti et al., 2009).

In urban/polluted areas, the particle size distribution is more complex (Lee et al., 2003; Alfarra et al., 2004; Zhang et al., 2004; Salcedo et al., 2006). Particle activation is affected by the composition and the mixing state of aerosol particles. It has been

demonstrated that particles are more difficult to activate during biomass burning plume events (Mircea et al., 2005; Lee et al., 2006; Clarke et al., 2007; Rose et al., 2010, 2011; Paramonov et al., 2013; Lathem et al., 2013). Also, their activation ratios are reduced by secondary organics formed from oxidation of common biogenic emissions (VanReken et al., 2005; Varutbangkul et al., 2006; Mei et al., 2013) and black carbon (Dusek et al., 2006b; Kuwata et al., 2007). Other organic components (e.g., organic acids) have been shown to activate more easily (Raymond and Pandis, 2002; Hartz et al., 2006; Bougiatioti et al., 2011), but still much less than inorganic species. Therefore, testing the understanding of parameters controlling CCN activation and growth is challenging in heavily polluted areas. Furthermore, the main uncertainty in predicting the magnitude of global aerosol indirect effects arises from those regions under the influence of urban emissions (Sotiropoulou et al., 2007). The study of aerosol-CCN closure and relationships within and in the outflow of heavily polluted areas is thus important.

East Asia, especially the Jing (Beijing)-Jin (Tianjin)-Ji (Hebei) region, is a fast developing and densely populated region including numerous megacities, where anthropogenic aerosol emissions have increased significantly over recent years (Streets et al., 2008) and where aerosol loading is high and chemical composition is complex (Li et al., 2007a; Xin et al., 2007). The high aerosol loading would have a significant influence on radiative properties, cloud microphysics, and precipitation (Xu, 2001; Li et al., 2007b; Xia et al., 2007; Rosenfeld et al., 2007; Lau et al., 2008; Li et al., 2011).

Field measurements of CCN have been made in East Asia where megacities are likely to be major sources of pollutants and CCN (Yum et al., 2007; Rose et al., 2010, 2011; Gunthe et al., 2009; Yue et al., 2011; Liu et al., 2011; Zhang et al., 2012; Deng et al.,

2011; Leng et al., 2013). Despite the significant accomplishments achieved by these studies, limitations and uncertainties exist. As a recent example over the region of interest, Deng et al. (2011) over-predicted concentrations of CCN at a site in the North China Plain by 19% when compared with direct measurements.

5 The aim of this paper is to study aerosol hygroscopicity and CCN activity under high aerosol loading conditions and to parameterize CCN number concentrations by using CCN activation ratios (AR) as a proxy of the total number of aerosol particles in the atmosphere. A cumulative Gaussian distribution function (CDF) fit model is applied to aerosol data collected under clean and polluted conditions to examine the influence
10 of size distribution, heterogeneity of chemical composition, and mixing state on CCN activity. The hygroscopicity parameter (κ) is derived using Köhler theory to study aerosol hygroscopicity on clean days and during polluted events. In the CCN closure study, in addition to the parallel observation (PO) closure test, we apply the CCN efficiency spectrum to non-simultaneous condensation nuclei (CN) and bulk CCN
15 observations, namely the non-parallel observation (NPO) closure test, to estimate N_{CCN} . Finally, the relationship between bulk AR and aerosol physical and chemical properties is examined.

2. Measurements and data

An intensive field campaign called the Aerosol-CCN-Cloud Closure Experiment
20 (AC³Exp) was conducted during June and July of 2013 at the Xianghe Atmospheric Observatory (39.798°N, 116.958°E; 35 m above sea level) located about 60 km southeast of the Beijing metropolitan area. This site is surrounded by agricultural land, densely occupied residences, and light industry. Sitting between two megacities (Beijing to the northwest and Tianjin to the southeast) and less than 5 km west of the
25 local town center (with a population of 50,000), the site experiences frequent

pollution plumes. Depending on the wind direction, instruments at the Xianghe site detect pollutants of urban, rural, or mixed origins, experiencing both fresh biomass burning emissions and advected aged aerosols. Details about the measurement location and meteorological conditions at the site can be found in Li et al. (2007, 5 2011).

2.1 Instruments and measurements

Bulk CCN activation was measured from 1 June to 25 June 2013. Size-resolved CCN were measured from 7 July to 21 July 2013. Aerosol particle size distributions (10-700 nm) were measured from 1 June to 25 June 2013 and from 7 July to 21 July 10 2013. During 1-25 June 2013, a Scanning Mobility Particle Sizer (SMPS) was used independently for size distribution measurements. From 7 July to 21 July 2013, it was combined with a Droplet Measurement Technologies - Cloud Condensation Nuclei Counter (DMT-CCNc) (Lance et al., 2006) and used for size-resolved CCN measurements. The CCN efficiency spectrum was derived from size-resolved CCN 15 observations made from 7 July to 21 July 2013. The aerosol particle size distribution data independently measured by the SMPS and bulk CCN measurements from 1 June to 25 June 2013 combined with the derived CCN efficiency spectrum (Fig. 1) is used for the NPO CCN closure test. Aerosol chemical composition was measured from 31 May to 30 June 2013.

20 The aerosol inlet for the size distribution measurements was equipped with a TSI Environmental Sampling System (Model 3031200), which consists of a standard PM10 inlet, a sharp-cut PM1 cyclone, and a bundled nafion dryer. After dried through the nafion bundle, the sample flow with relative humidity (RH) of < 30% was sent into the SMPS for the aerosol size distribution measurements (10-700 nm).

Meanwhile, the bulk N_{CCN} at different SS was measured, using a continuous-flow CCN counter from the DMT-CCN_C. Each bulk CCN measurement cycle included three SS levels: 0.23%, 0.51% and 0.80%. The scanning times for those SS levels were set at 7, 5, and 5 minutes, respectively.

- 5 The size-resolved CCN efficiency spectra were measured by coupling the same DMT-CCN_C used with the SMPS (Rose et al., 2008). In this setup the particles are rapidly dried with $RH < 30\%$ upon entering the Differential Mobility Analyzer (DMA). Thus, size selection is effectively performed under dry conditions, and the relative deviations in particle diameter should be $< 1\%$ except for potential kinetic
- 10 limitations (Mikhailov et al., 2009). The sample flow exiting the DMA was split into two parts, with 0.3 lpm for the CPC and 0.5 lpm for the CCN_C. The DMA, controlled by the TSI-AIM software, scanned one size distribution every five minutes. The CCN_C was operated at a total flow rate of 0.5 lpm with a sheath-to-aerosol flow ratio of 10. The inlet RH for CCN_C was $< 30\%$. During the field campaign, the mean
- 15 sample temperature and pressure measured by the CCN_C sensors were $(23.5 \pm 1.6) ^\circ\text{C}$ and $(985.5 \pm 3.6) \text{ hPa}$. The SS levels of CCN_C were calibrated with ammonium sulfate before and after the field campaign, following procedures outlined in Rose et al. (2008). During each CCN measurement cycle, calibrated effective SS are 0.08%, 0.11%, 0.23%, 0.42%, and 0.80%. The overall error (1σ) for the SS levels was
- 20 estimated to be $< 3.5\%$. The completion of a full measurement cycle took 60 min (20 min for SS = 0.08% and 10 min for the other SS levels).

The measurement of non-refractory submicron aerosol species including organics, sulfate, nitrate, ammonium, and chloride were made with an Aerodyne Aerosol Chemical Speciation Monitor (ACSM) (Sun et al., 2012). The ACSM uses the same

25 aerosol sampling, vaporization and ionization modules as the Aerosol Mass

Spectrometer (AMS) (DeCarlo et al., 2006), but removes the size components. During the field campaign, ambient aerosols were drawn inside through a ½ inch (outer diameter) stainless steel tube at a flow rate of ~3 L min⁻¹, of which ~84 cc min⁻¹ was sub-sampled into the ACSM. An URG cyclone (Model: URG-2000-30ED) was also
5 supplied in front of the sampling inlet to remove coarse particles with a size cut-off of 2.5 mm. Before sampled into the ACSM, aerosol particles are dried by Silica gel desiccant. The residence time in the sampling tube is ~5 s. The ACSM was operated at a time resolution of ~15 min with a scan rate of mass spectrometer at 500 ms amu⁻¹ from m/z 10 to 150. Regarding the calibration of the ACSM, mono-dispersed,
10 size-selected 300 nm ammonium nitrate particles within a range of concentrations were sampled into both the ACSM and a condensation particle counter (CPC). The ionization efficiency (IE) was then determined by comparing the response factors of the ACSM to the mass calculated with known particle size and number concentrations from the CPC. Once the IE is determined, changes in the internal standard
15 naphthalene or air ions, e.g., m/z 28 (N₂⁺) or m/z 32 (O₂⁺), can be used to account for the degradation of the detector. Other details including the instrument, aerosol sampling setup, operations, and calibration are given in Sun et al. (2012) and Ng et al. (2011).

In addition to the ACSM, the black carbon (BC) in PM_{2.5} was simultaneously
20 measured at a time resolution of 5 min by a BC analyzer (Aethalometer, Model AE22, Magee Scientific Corporation). The campaign averaged mass concentrations of BC are ~4.2 µg m⁻³, and the averaged mass fraction is about 6%, with maximum of 18% and minimum of 2%. During the experiment period, the campaign area was generally hot and moist, with an average temperature of 23.6 °C and an average ambient RH of
25 72.3%.

2.2 Data

The raw CCN data for both bulk and size-resolved CCN measurements were first filtered according to the instrument recorded parameters (e.g., temperature and flow). For example, if the relative difference between the actual and set sample flows was larger than 4%, the data are flagged as invalid data. If the “Temp. Stability” was recorded as “0”, the data is also flagged as invalid data due to instrument fluctuations. These flagged data are not used for further analysis. A multiple charge correction and transfer function (Deng et al., 2011) is applied to each CN size distribution spectrum as well as to the CCN efficiency spectrum. The CCN AR is the ratio of N_{CCN}/N_{CN} . To examine CCN activity under different conditions, the size-resolved CCN efficiency data was classified as polluted or as background based on the aerosol loading as well as the synchronal surface horizontal wind data. Polluted conditions are identified when the total CN number concentration (N_{CN}) $> 15000 \text{ cm}^{-3}$ and when the airflow came from southeast/east. Background cases are identified when $N_{CN} < 15000 \text{ cm}^{-3}$ and when winds were from the west or northwest. N_{CN} is the total aerosol number concentration with a particle size range of 10-700 nm. Here, the background refers to a regional background condition which represents a well-mixed atmosphere unaffected by local emissions, e.g., biomass burning. Bulk measurements of total CCN number concentrations at SS levels of 0.23%, 0.51% and 0.80% could lead to a considerable underestimation of N_{CCN} under polluted conditions (Deng et al., 2011) due to water depletion inside the column (Lathem and Nenes, 2011). Therefore, in this study, data points with $N_{CN} > 25000 \text{ cm}^{-3}$ were excluded. In the closure study, CCN size distributions were calculated by multiplying the fitted campaign-averaged CCN efficiency spectrum (a 3-parameter CDF fit) with the aerosol particle number size distribution. The total N_{CCN} was then obtained by integrating the size-resolved N_{CCN}

over the whole size range. Aerosol mass concentrations were processed using ACSM standard data analysis software (version 1.5.1.1). Detailed procedures for the data analysis have been described in Ng et al. (2011) and Sun et al. (2012).

3. Theory

5 As proposed by Petters and Kreidenweis (2007), κ can be used to describe the ability of particles to absorb water vapor and act as CCN. Based on Köhler theory (Köhler, 1936), κ relates the dry diameter of aerosol particles to the critical water vapor SS. According to measurements and thermodynamic models, κ is zero for insoluble materials like soot or mineral dust. However, their hygroscopicity changes due to the
10 aging process, so the κ value then is > 0 . The magnitude of κ is ~ 0.1 for secondary organic aerosols, ~ 0.6 for ammonium sulfate and nitrate, 0.95-1 for sea salt (Niedermeier et al., 2008), and 1.28 for sodium chloride aerosols. The effective hygroscopicity of mixed aerosols can be approximated by a linear combination of the κ -values of the individual chemical components weighted by the volume or mass
15 fractions (Kreidenweis et al., 2008; Gunthe et al., 2009). In this study, we calculated κ based on both size-resolved CCN measurements and bulk chemical composition observations made during the field campaign. The method to derive κ is described below.

3.1 Derivation of κ_a

20 The magnitude of κ was derived from the measured size-resolved CCN activated fraction using κ -Köhler theory (Petters and Kreidenweis, 2007). In κ -Köhler theory, the water vapor saturation ratio over an aqueous solution droplet S_c is given by:

$$S_c = \frac{D^3 - D_p^3}{D^3 - D_p^3(1 - \kappa)} \exp\left(\frac{4\sigma_w M_w}{RT \rho_w D}\right) \quad (1)$$

where D is the droplet diameter, D_p is the dry diameter of the particle, M_w is the molecular weight of water, σ_w is the surface tension of pure water, ρ_w is the density of water, R is the gas constant, and T is the absolute temperature. When κ is greater than 5 0.1, it can be conveniently expressed as:

$$\kappa = \frac{4A^3}{27D_p^3 S_c^2} \quad (2)$$

$$A = \frac{4\sigma_w M_w}{RT \rho_w D} \quad (3)$$

where S_c is the particle critical supersaturation and is derived using the approach described by Rose et al. (2008). The characteristic S_c of the size selected CCN is 10 represented by the SS level at which AR reaches 50%. For the parameters listed above, $T = 298.15$ K, $R = 8.315$ J K⁻¹ mol⁻¹, $\rho_w = 997.1$ kg m⁻³, $M_w = 0.018015$ kg mol⁻¹, and $\sigma_w = 0.072$ J m⁻². Note that values derived from CCN measurement data through Köhler model calculations assuming the surface tension of pure water have to be regarded as “effective hygroscopicity parameters” that account not only for the 15 reduction of water activity by the solute (“effective Raoult parameters”) but also for surface tension effects (Petters and Kreidenweis, 2007). In this study, a parameter called κ_a , which characterizes the average hygroscopicity of CCN-active particles in the size range around activated diameters (D_a), is calculated from the data pairs of SS and D_a based on the κ -Köhler theory.

20 3.2 Derivation of κ_{chem}

For a given internal mixture, κ can be predicted by a simple mixing rule on the basis of chemical volume fractions, ε_i (Petters and Kreidenweis, 2007; Gunthe et al., 2009):

$$\kappa_{chem} = \sum_i \varepsilon_i \kappa_i \quad (4)$$

where κ_i and ε_i are the hygroscopicity parameter and volume fraction for the individual (dry) components in the mixture and i is the number of components in the mixture. We derive ε_i from the particle chemical composition measured by the ACSM. Measurements from the ACSM show that the composition of submicron particles was dominated by organics, followed by nitrate, ammonium, and sulfate. The contribution of chloride was negligible (with a volume fraction of about < 2%). The analysis of the anion and cation balance suggests that anionic species (NO_3^- , SO_4^{2-}) were essentially neutralized by NH_4^+ over the relevant size range. For refractory species, BC represented a negligible fraction of the total submicron aerosol volume (less than 3%). Sea salt and dust are usually coarse mode particles with particle sizes > 1 μm (Whitby, 1978). The contribution of such types of aerosols is thus expected to be negligible for sizes < 1000 nm. Therefore, the submicron particles measured by the ACSM mainly consisted of organics, $(\text{NH}_4)_2\text{SO}_4$, and NH_4NO_3 . The particle hygroscopicity is thus the volume average of the three participating species:

$$\kappa_{chem} = \kappa_{Org}\varepsilon_{Org} + \kappa_{(\text{NH}_4)_2\text{SO}_4}\varepsilon_{(\text{NH}_4)_2\text{SO}_4} + \kappa_{\text{NH}_4\text{NO}_3}\varepsilon_{\text{NH}_4\text{NO}_3} \quad (5)$$

The values of κ are 0.67 and 0.61 for $(\text{NH}_4)_2\text{SO}_4$ and NH_4NO_3 , respectively, which are derived from previous laboratory experiments (Petters and Kreidenweis, 2007). The following linear function derived by Mei et al. (2013) was used to estimate κ_{Org} in our study: $\kappa_{Org} = 2.10 \times f_{44} - 0.11$. The mean value of κ_{Org} during the field campaign is 0.115 ± 0.019 . Species volume fractions were derived from mass concentrations and densities of participating species. The densities of $(\text{NH}_4)_2\text{SO}_4$ and NH_4NO_3 are 1770 kg m^{-3} and 1720 kg m^{-3} , respectively. The density of organics is 1200 kg m^{-3} (Turpin et al., 2001).

4. Results and discussion

4.1 CDF fit and parameters derived from the CCN efficiency

The spectra of measured CCN efficiency under both polluted and background conditions were fitted with a CDF (Rose et al., 2008):

$$f_{N_{CCN}/N_{CN}} = a \left(1 + \operatorname{erf} \left(\frac{D - D_a}{\sigma_a \sqrt{2}} \right) \right) \quad (6)$$

where the maximum activated fraction (*MAF*), is equal to $2a$, D_a is the midpoint activation diameter, and σ_a is the CDF standard deviation. These parameters were determined for each spectrum. If $MAF=1$ by changing the parameter “ a ” to 0.5, the spectrum is characteristic for internally mixed aerosols with homogeneous composition and hygroscopicity. The 3-parameter fit results represent the average activation properties of the aerosol particle fraction. During the field campaign, about 1200 size-resolved CCN efficiency spectra for atmospheric aerosols at SS levels of 0.08% to 0.80% were measured. Figure 1 shows campaign-averaged spectra of both measured and fitted CCN efficiency at SS levels of 0.08%, 0.11%, 0.23%, 0.42%, and 0.80% for background and polluted conditions. The slope of AR with respect to diameters near D_a in Fig. 1 provides information about the heterogeneity of the composition for the size-resolved particles. For an ideal case when all CCN-active particles have the same composition and size, a steep change of AR from 0 to *MAF* would be observed as D reaches D_a . A gradual increase in size-resolved AR with particle diameter suggests that aerosol particles consisted of different hygroscopicities. The gentler slopes of AR around D_a during polluted events show that the particle composition was more heterogeneous than the particle composition under background conditions. Significant differences in size-resolved CCN efficiency spectra under polluted and clean conditions at lower SS levels have been derived. The different

shapes suggest that aerosol hygroscopicity and CCN activity would be affected by local emission sources, e.g., biomass burning.

4.1.1 Activation diameter (D_a)

The three parameters (MAF , D_a , and σ) describing the CCN efficiency spectra derived from the 3-parameter CDF fits, as well as κ_a under polluted and clean conditions, are summarized in Table 1. Activation diameters under polluted and clean conditions are denoted as D_{a_POL} and D_{a_BG} in Table 1, respectively. As expected, D_a decreases with increasing SS under both background and polluted conditions. At a given SS, D_{a_POL} is greater than D_{a_BG} , suggesting that particles under polluted conditions would be activated at a larger diameter. As SS increases, the difference between D_{a_POL} and D_{a_BG} decreases.

4.1.2 Maximum Activated Fraction (MAF)

In general, aerosols with a more uniform and homogenous chemical composition or with a core-shell structure would have a higher MAF . The MAF under polluted and background conditions is denoted by MAF_POL and MAF_BG in Table 1, respectively. Values of MAF_BG and MAF_POL range from 0.95-0.98 and from 0.94-0.98, respectively. No significant discrepancies in MAF are observed between polluted and background conditions. Observations show that particles can activate to CCN completely when particle diameters are greater than 300 nm even at SS = 0.08%. This suggests that a smaller portion of $1-MAF$ (2-6%) is caused by the error in the CDF fit, which will lead to a lower MAF than expected.

4.1.3 CDF standard deviations (σ)

CDF standard deviations (σ) are general indicators for the extent of external mixing and the heterogeneity of particle composition for aerosols in the size range around D_a . CDF σ under polluted and background conditions are denoted as σ_{POL} and σ_{BG} in Table 1, respectively. Under ideal conditions, σ equals zero for an internally mixed, fully mono-dispersed aerosol with particles of homogeneous chemical composition. According to [Rose et al. \(2008\)](#), even after correcting for the DMA transfer function, calibration aerosols composed of high-purity ammonium sulfate exhibit small non-zero σ values that correspond to $\sim 3\%$ of D_a . This can be attributed to heterogeneities of the water vapor SS profile in the CCNC or other non-idealities, such as DMA transfer function and particle shape effects. Thus, “heterogeneity parameter” values of $\sigma/D_a = 3\%$ indicate internally mixed CCN, whereas higher values indicate external mixtures of particles. Heterogeneity parameters under polluted and background conditions are denoted as σ/Da_{POL} and σ/Da_{BG} in Table 1, respectively. They range from 17%-30%, which is much higher than the 3% observed for pure ammonium sulfate, indicating that the particles were externally mixed with respect to their solute content.

4.2 Derived κ_a dependence on D_a

Figure 2 shows the dependence of κ_a on D_a under background and polluted conditions. $\kappa_{a_{POL}}$ and $\kappa_{a_{BG}}$ are defined as the average hygroscopicity of CCN-active particles in the size range around D_a under polluted and background conditions, respectively. For background days, larger particles were on average more hygroscopic than smaller particles, i.e., $\kappa_{a_{BG}}$ increases substantially from about 0.22 at 30-60 nm to about 0.38 at the size range of 120-180 nm. This is consistent with field results observed in

Guangzhou, South China by Rose et al. (2010). However, compared to κ_{a_BG} , κ_{a_POL} shows a relatively flat trend as the particle size diameter increases and error bars are larger. This suggests that under polluted conditions, particle composition and their mixing state is complex and diverse. In this case, larger particles are even less
5 hygroscopic than smaller particles. One possible reason for changes in κ_a under polluted conditions may be the presence of high amount of organics freshly emitted from biomass burning (Andreae and Rosenfeld, 2008; Petters et al., 2009; Rose et al., 2010) which would coat the larger particles and render them less hygroscopic. Overall, κ for polluted aerosols are about 20% lower than that for clean aerosols for particles in
10 the accumulation size range. For particles in the nucleation or Aitken size range, κ_a for polluted particles is slightly higher than that for particles in the background cases. Based on laboratory experiments, Petters et al. (2009) examined the hygroscopic properties of particles freshly emitted from biomass burning. They found that κ was a function of particle size, with 250 nm particles being generally weakly hygroscopic
15 and sub-100 nm particles being more hygroscopic. During the field campaign, polluted cases represent cases where particles were mainly biomass burning aerosols. The laboratory results, to some extent, can thus explain our field measurements. Further investigations, including laboratory experiments and field measurements of size-resolved chemical composition, are needed to confirm and clarify this.

20 4.4 PDF of D_a and κ_a

Figure 3 shows probability distribution functions (PDF) of D_a under background conditions and during polluted events. D_{a_POL} are mainly distributed in the ranges of about 185-205, 163-180, 95-120, 65-75 and 45-55 nm at SS levels of 0.08%, 0.11%, 0.23%, 0.42% and 0.80%, respectively. At each SS level, the PDFs of D_{a_POL} have a

wider distribution than the PDFs of D_{a_BG} . At each SS level, the PDFs of D_{a_POL} extend to large particle sizes indicating the impact by pollution. The largest variation in D_{a_BG} and D_{a_POL} is seen at SS = 0.08% and 0.11%, respectively. One reason for this is the weakened impact of chemical composition on CCN activity at high SS levels, i.e., the solute effect. The other reason is the relatively larger uncertainties that arise from making measurements at low SS levels.

Figure 4 shows PDFs of κ_a under background conditions and during polluted events. The PDF of κ_{a_POL} has a large variation at each size range around D_p and shows two modes. For example, κ_{a_POL} for particles around 48 nm shows two peaks at ~0.15 and ~0.23. Peak values of ~0.26 and ~0.32 are seen for particles around $D_p = 198$ nm. Most κ_{a_POL} values are less than 0.3. This suggests externally mixed, but less hygroscopic particles during polluted events. Less variation is seen in the PDFs of κ_{a_BG} . One mode is seen with peak values of 0.23, 0.30, 0.35, 0.35, and 0.38 for $D_p = 46, 64, 92, 152,$ and 179 nm, respectively. Most κ_{a_BG} values are greater than 0.3 when $D_p > 60$ nm, indicating that the particles are more hygroscopic with a relatively homogeneous composition.

4.5 CCN closure tests

In this section, we compare observed total N_{CCN} with corresponding values that were estimated on the basis of aerosol particle number size distributions measured in parallel and not in parallel and assuming a uniform particle composition. Closure is achieved if estimated and observed N_{CCN} agree quantitatively within the range of their uncertainties.

4.5.1 PO closure test

In PO closure tests, the measured CCN efficiency spectrum is first multiplied by the

measured CN size distribution, which yields the CCN size distribution. This is then integrated over the whole size range to obtain the observed total CCN concentration (CCN_Obs). Size-resolved N_{CCN} are calculated by multiplying the campaign-averaged CCN efficiency spectrum with simultaneously measured CN number size distributions.

5 Estimated total N_{CCN} (CCN_Estimated) are obtained by the stepwise integration of size-resolved N_{CCN} from 10 to 700 nm. With this comparison, the influence of the variation in chemical composition on the CCN concentration can be investigated because the CN size distribution is the same for both parameters.

Fig. 5 shows CCN_Estimated as a function of CCN_Obs. at SS levels ranging from
10 0.08% to 0.80%. Estimated and measured total N_{CCN} agree well. The mean slope and correlation coefficient (R^2) are 0.99 and 0.97, respectively, at the five SS levels. A ~3-4% underestimation occurs at SS levels of 0.08% and 0.11%. One reason for this slight underestimation is that size-resolved ARs are more variable at low SS levels than at higher SS levels. Also, compared to total activated CCN number
15 concentrations at high SS levels, there are less N_{CCN} at low SS levels, which would lead to larger uncertainties or to a lower correlation. Overall, CCN closure can be achieved by using campaign-averaged CCN efficiency spectra. In this PO closure test, the influence of variations in chemical composition on CCN concentrations is insignificant.

20 **4.5.2 NPO closure test**

Mean CCN efficiency spectra derived from size-resolved CCN measurements taken on 7-21 July 2013 are used to estimate total CCN number concentrations based on CN size distribution measurements taken on 1-25 June 2013. This is referred to as an NPO closure test. The average measured CCN efficiency spectrum (corresponding to

spectra in Fig. 1) is multiplied by the measured CN size distribution which yields the CCN size distribution. This is integrated over the whole size range (10-700 nm) to obtain the estimated total CCN concentration. The mean CCN efficiency spectra at SS levels of 0.23% and 0.80% (Fig. 1) is used to estimate the total CCN concentration during 1-25 June 2013. The mean CCN efficiency spectra at SS = 0.51% is derived using the exponential relationships developed from plotting the three CDF fit parameters as a function of SS (see Fig. 7).

Estimated total N_{CCN} as a function of measured bulk N_{CCN} at SS levels of 0.23%, 0.51%, and 0.80% are shown in Fig. 6. The lower slope at SS = 0.23% indicates that the estimation on the basis of NPO closure underestimates about 7% of the observed N_{CCN} . The closure is considerably improved at higher SS levels. A reasonable correlation between estimated and measured total N_{CCN} is seen ($R^2 = 0.6-0.8$), which suggests temporal variations in chemical composition and mixing state of aerosol particles. In addition, there are uncertainties due to measuring bulk and size-resolved CCN. Overall, uncertainties in this NPO CCN closure study range from 30%-40%. Caution is needed when using data from any short-term experiment at a single site to do CCN parameterizations for large-scale applications. It is necessary to conduct long-term CCN measurements at more regional sites, especially those that are heavily polluted.

20 **4.6 Case study: CCN activation and chemical composition**

The behavior of CCN activation under background and polluted conditions is examined. Two cases are selected: one case with total $N_{\text{CN}} < 15000 \text{ cm}^{-3}$ (background) and another case with total $N_{\text{CN}} > 15000 \text{ cm}^{-3}$ (polluted). Trends in bulk CCN activation as N_{CN} increases are different for the background and polluted cases. Bulk

AR at the three SS levels (0.23%, 0.51%, and 0.80%) increases as total N_{CN} increases for background cases (Fig. 8a) and decreases as total N_{CN} increases for polluted cases (Fig. 8b). For the background cases, changes in bulk AR are dependent on changes in κ_{chem} (Fig. 8c). A good correlation between AR_{0.23} and κ_{chem} ($R^2 > 0.7$) is seen in Fig. 9. A high correlation between bulk AR and κ_{chem} when total N_{CN} is low has been observed during the campaign (Fig. 10). In these cases, organics account for ~30% of the total particle mass concentration and concentrations of soluble inorganics are high (Fig. 8e). In particular, the mass concentration of nitrate is higher than that for organics and accounts for the largest mass fraction when κ_{chem} reaches a maximum with a mean value of ~0.45. The f_{44} , which is the fraction of total organic mass signal at m/z 44, is not correlated with AR (Fig. 8c). The m/z 44 signal is mostly due to acids (Takegawa et al., 2007; Duplissy et al., 2011) or acid-derived species, such as esters, and f_{44} is closely related to the organic oxidation level, i.e., O:C ratio (Aiken et al., 2008). Oxidized/aged acids are generally more hygroscopic and easily activated. Therefore, the lower correlation between f_{44} and AR implies that organics under low N_{CN} conditions are less hygroscopic. CN number concentrations in the nucleation, Aitken, and accumulation modes are shown in Fig. 8g (polluted) and Fig. 8h (background). Under background conditions, bulk AR at SS = 0.23% is more correlated ($R^2 = 0.5$) with changes in N_{CN} in the accumulation mode (Fig. 9), suggesting that most aerosol particles with sizes > 100 nm can be activated. Smaller particles with Aitken diameters of < 40 nm at the given SS levels (0.23%-0.80%) are not as easily activated, if at all, so no correlation is seen (Fig. 8g).

Under polluted conditions, there is little dependence of changes in bulk AR with changes in κ_{chem} (Fig. 8d). Bulk AR at SS = 0.23% is moderately correlated with f_{44} ($R^2 = 0.5$, Fig. 9). As stated above, f_{44} is always related to the organic oxidation level.

Usually, oxidized/aged acids are more hygroscopic and easily activated. The correlation between f_{44} and bulk AR suggests that the organics contribution from oxidized or aged aerosols play a significant role in CCN activity (Jimenez et al., 2009). A bias is introduced by using a parameterized function derived from observations made at other sites with different aerosol types to describe the particle hygroscopicity and activation properties due to the complexity of the organic aerosol fraction and its tendency to evolve with atmospheric oxidative processing and aerosol aging (e.g., Padró et al., 2010; Engelhart et al., 2011, 2012; Asa-Awuku et al., 2011). Under polluted conditions, the bulk AR_{0.2} is more correlated with changes in accumulation mode particles ($R^2 = \sim 0.3$).

Overall, based on the case study, one cannot use a parameterized formula using only total N_{CN} to estimate total CCN number concentrations. If observations such as size-resolve CCN and size-resolved chemical composition are not available, the possibility of using bulk κ_{chem} and f_{44} in combination with bulk $N_{\text{CN}} > 100$ nm to parameterize CCN number concentrations is implied by the case study. Further field investigations are needed to demonstrate and confirm the relationship between bulk AR and particle size and composition.

5. Summary and conclusions

Atmospheric aerosol particles acting as CCN are pivotal elements of the hydrological cycle and climate change. In this study, we measured and characterized N_{CCN} in relatively clean and polluted air during the AC³Exp campaign conducted at Xianghe, China during summer 2013. The aim was to examine CCN activation properties under high aerosol loading conditions in a polluted region and to assess the impacts of particle size and chemical composition on the CCN AR which acts as a proxy of the total number of aerosol particles in the atmosphere. Based on the CDF fit method, a

gradual increase in size-resolved AR with particle diameter suggests that aerosol particles have different hygroscopicities. D_a increased significantly at lower SS levels (< 0.23%) due to pollution, e.g., biomass burnings. This increase was not observed when SS > 0.4%. For particles in the accumulation mode, values of κ range from 0.31-0.38 under background conditions, which is about 20% higher than that derived under polluted conditions. For particles in the nucleation or Aitken mode, κ range from 0.20-0.34 under both background and polluted conditions. Larger particles were on average more hygroscopic than smaller particles. However, the case is more complex for particles originating from heavy pollution due to the diversity in particle composition and mixing state. The low R^2 for the NPO CCN closure test suggests a 30%-40% uncertainty in total N_{CCN} estimation. Using bulk chemical composition data from ACSM measurements, the relationship between bulk AR and the physical and chemical properties of atmospheric aerosols is investigated. Based on a case study, we conclude that one cannot use a parameterized formula using only total N_{CN} to estimate total N_{CCN} . We have shown the possibility of using bulk κ_{chem} and f_{44} in combination with bulk $N_{CN} > 100$ nm to parameterize CCN number concentrations. Further field investigations or examinations are needed to demonstrate and confirm the relationship between bulk AR and particle size and composition.

Acknowledgements

We thank the reviewers for their suggestions and comments which have greatly improved the paper. This work was funded by the National Basic Research Program of China '973' (Grant No. 2013CB955801, 2013CB955804), the National Science Foundation (1118325), and the Fundamental Research Funds for the Central Universities (Grant No. 2013YB35). We greatly appreciate the support of the entire AC³Exp team.

References

- Aiken, A. C., DeCarlo, P. F., Kroll, J. H., Worsnop, D. R., Huffman, J. A., Docherty, K. S., Ulbrich, I. M., Mohr, C., Kimmel, J. R., Sueper, D., Sun, Y., Zhang, Q., Trimborn, A., Northway, M., Ziemann, P. J., Canagaratna, M. R., Onasch, T. B.,
5 Alfarra, M. R., Prevot, A. S. H., Dommen, J., Duplissy, J., Metzger, A., Baltensperger, U., and Jimenez, J. L.: O/C and OM/OC ratios of primary, secondary, and ambient organic aerosols with high-resolution time-of-flight aerosol mass spectrometry, *Environ. Sci. Technol.*, 42, 4478–4485, 2008.
- Albrecht, B. A.: Aerosols, clouds and microphysics, *Science*, 245, 1227–1230, 1989.
- 10 Alfarra, M. R., Coe, H., Allan, J. D., Bower, K. N., Boudries, H., Canagaratna, M. R., Jimenez, J. L., Jayne, J. T., Garforth, A. A., Li, S.-M., and Worsnop, D. R.: Characterization of urban and rural organic particulate in the Lower Fraser Valley using two Aerodyne Aerosol Mass Spectrometers., *Atmos. Environ.*, 38, 5745–5758, 2004.
- 15 Andreae, M. O. and Rosenfeld, D.: Aerosol-cloud precipitation interactions. Part 1. The nature and sources of cloud-active aerosols, *Earth. Sci. Rev.*, 89, 13-41, doi:10.1016/j.earscirev.2008.03.001, 2008.
- Anttila, T. and Kerminen, V. M.: On the contribution of Aitken mode particles to cloud droplet populations at continental background areas – a parametric sensitivity
20 study, *Atmos. Chem. Phys.*, 7, 4625–4637, 2007.
- Asa-Awuku, A., Moore, R. H., Nenes, A., Bahreini, R., Holloway, J. S., Brock, C. A., Middlebrook, A. M., Ryerson, T., Jimenez, J., DeCarlo, P., Hecobian, A., Weber, R., Stickel, R., Tanner, D. J., and Huey, L. G.: Airborne cloud condensation nuclei measurements during the 2006 Texas Air Quality Study, *J. Geophys. Res.*, 116,
25 D11201, doi:10.1029/2010JD014874, 2011.

- Bougiatioti, A., Fountoukis, C., Kalivitis, N., Pandis, S. N., Nenes, A., and Mihalopoulos, N.: Cloud condensation nuclei measurements in the marine boundary layer of the eastern Mediterranean: CCN closure and droplet growth kinetics. *Atmos. Chem. Phys.*, 9, 7053–7066, 2009.
- 5 Bougiatioti, A., Nenes, A., Fountoukis, C., Kalivitis, N., Pandis, S. N., and Mihalopoulos, N.: Size-resolved CCN distributions and activation kinetics of aged continental and marine aerosol, *Atmos. Chem. Phys.*, 11, 8791–8808, doi:10.5194/acp-11-8791-2011, 2011.
- Chuang, P. Y., Collins, D. R., Pawlowska, H., Snider, J. R., Jonsson, H. H., Brenguier, J. L., Flagan, R. C., and Seinfeld, J. H.: CCN measurements during ACE-2 and their relationship to cloud microphysical properties, *Tellus B*, 52, 843–867, 2000.
- 10 Clarke, A., McNaughton, C., Kasputin, V. N., Shinozuka, Y., Howell, S., Dibb, J., Zhou, J., Anderson, B., Brekhovskikh, V., Turner, H., and Pinkerton, M.: Biomass burning and pollution aerosol over North America: Organic components and their influence on spectral optical properties and humidification response, *J. Geophys. Res.*, 112, D12S18, doi:10.1029/2006JD007777, 2007.
- 15 DeCarlo, P.F., Kimmel, J.R., Trimborn, A., Northway, M.J., Jayne, J.T., Aiken, A.C., Gonin, M., Fuhrer, K., Horvath, T., Docherty, K.S., Worsnop, D.R., Jimenez, J.L.: Field-deployable, high-resolution, time-of-flight aerosol mass spectrometer. *Anal. Chem.*, 78, 8281–8289, 2006.
- 20 Deng, Z., Zhao, C., Ma, N., Liu, F., Ran, L., Xu, W., Liang, Z., Liang, S., Huang, M., Ma, X., Zhang, Q., Quan, J., and Yan, P.: Size-resolved and bulk activation properties of aerosols in the North China Plain. *Atmos. Chem. Phys.*, 11, 3835–3846, 2011.
- 25 Deng, Z., Zhao, C., Ma, N., Ran, L., Zhou, G., Lu, D., and Zhou, X.: An examination

of parameterizations for the CCN number concentration based on in situ measurements of aerosol activation properties in the North China Plain, *Atmos. Chem. Phys.*, 13, 6227–6237, doi:10.5194/acp-13-6227-2013, 2013.

Dusek, U., Covert, D. S., Wiedensohler, A., Neususs, C., Weise, D., and Cantrell, W.:

5 Cloud condensation nuclei spectra derived from size distributions and hygroscopic properties of the aerosol in coastal south-west Portugal during ACE-2, *Tellus B*, 55, 35–53, 2003.

Dusek, U., Frank, G. P., Hildebrandt, L., Curtius, J., Schneider, J., Walter, S., Chand, D., Drewnick, F., Hings, S., Jung, D., Borrmann, S., and Andreae, M. O.: Size

10 matters more than chemistry for cloud-nucleating ability of aerosol particles, *Science*, 312, 1375–1378, 2006a.

Dusek, U., Reischl, G. P., and Hitzenberger, R.: CCN activation of pure and coated carbon black particles, *Environ. Sci. Technol.*, 40, 1223–1230, 2006b.

Duplissy, J., DeCarlo, P. F., Dommen, J., Alfarra, M. R., Metzger, A., Barmpadimos,

15 I., Prevot, A. S. H., Weingartner, E., Tritscher, T., Gysel, M., Aiken, A. C., Jimenez, J. L., Canagaratna, M. R., Worsnop, D. R., Collins, D. R., Tomlinson, J., and Baltensperger, U.: Relating hygroscopicity and composition of organic aerosol particulate matter, *Atmos. Chem. Phys.*, 11, 1155–1165, doi:10.5194/acp-11-1155-2011, 2011.

20 Engelhart, G. J., Moore, R. H., Nenes, A., and Pandis, S. N.: Cloud condensation nuclei activity of isoprene secondary organic aerosol, *J. Geophys. Res.*, 116, D02207, doi:10.1029/2010JD014706, 2011.

Engelhart, G. J., Hennigan, C. J., Miracolo, M. A., Robinson, A. L., and Pandis, S. N.:

25 Cloud condensation nuclei activity of fresh primary and aged biomass burning aerosol, *Atmos. Chem. Phys.*, 12, 7285–7293, doi:10.5194/acp-12-7285-2012,

2012.

Ervens, B., Feingold, G., and Kreidenweis, S.: Influence of watersoluble organic carbon on cloud drop number concentration., *J. Geophys. Res.*, 110, D18211, doi:10.1029/2004JD005634, 2005.

5 Feingold, G.: Modeling of the first indirect effect: Analysis of measurement requirements, *Geophys. Res. Lett.*, 30(19), doi:10.1029/2003GL017967, 2003.

Gasparini, R., Collins, D. R., Andrews, E., Sheridan, P. J., Ogren, J. A., and Hudson, J. G.: Coupling aerosol size distributions and size-resolved hygroscopicity to predict humidity-dependent optical properties and cloud condensation nuclei spectra., *J. Geophys. Res.*, 111, D05S13, doi:10.1029/2005JD006092, 2006.

10

Gunthe, S. S., King, S. M., Rose, D., Chen, Q., Roldin, P., Farmer, D. K., Jimenez, J. L., Artaxo, P., Andreae, M. O., Martin, S. T., and Pöschl, U.: Cloud condensation nuclei in pristine tropical rainforest air of Amazonia: size-resolved measurements and modeling of atmospheric aerosol composition and CCN activity, *Atmos. Chem. Phys.*, 9, 7551-7575, doi:10.5194/acp-9-7551-2009, 2009.

15

Hartz, K. E. H., Tischuk, J. E., Chan, M. N., Chan, C. K., Donahue, N. M., and Pandis, S. N.: Cloud condensation nuclei activation of limited solubility organic aerosol, *Atmos. Environ.*, 40, 605–617, 2006.

Hudson, J.: Variability of the relationship between particle size and cloud-nucleating ability, *Geophys. Res. Lett.*, 34, L08801, doi:10.1029/2006GL028850, 2007.

20

IPCC: Climate change 2007: Scientific basis, Fourth assessment of the Inter-governmental Panel on Climate Change, Cambridge Univ. Press, New York, 2007.

IPCC: Climate change 2013: Scientific basis, Fifth assessment of the Inter-governmental Panel on Climate Change, Cambridge Univ. Press, New York,

25

2013.

- Jimenez, J. L., Canagaratna, M. R., Donahue, N. M., Prevot, A. S. H., Zhang, Q., Kroll, J. H., DeCarlo, P. F., Allan, J. D., Coe, H., Ng, N. L., Aiken, A. C., Docherty, K. S., Ulbrich, I. M., Grieshop, A. P., Robinson, A. L., Duplissy, J., Smith, J. D.,
5 Wilson, K. R., Lanz, V. A., Hueglin, C., Sun, Y. L., Tian, J., Laaksonen, A., Raatikainen, T., Rautiainen, J., Vaattovaara, P., Ehn, M., Kulmala, M., Tomlinson, J. M., Collins, D. R., Cubison, M. J., Dunlea, E. J., Huffman, J. A., Onasch, T. B., Alfarra, M. R., Williams, P. I., Bower, K., Kondo, Y., Schneider, J., Drewnick, F., Borrmann, S., Weimer, S., Demerjian, K., Salcedo, D., Cottrell, L., Griffin, R.,
10 Takami, A., Miyoshi, T., Hatakeyama, S., Shimono, A., Sun, J. Y., Zhang, Y. M., Dzepina, K., Kimmel, J. R., Sueper, D., Jayne, J. T., Herndon, S. C., Trimborn, A. M., Williams, L. R., Wood, E. C., Middlebrook, A. M., Kolb, C. E., Baltensperger, U., and Worsnop, D. R.: Evolution of Organic Aerosols in the Atmosphere, *Science*, 326, 1525–1529, 2009.
- 15 Köhler, H.: The nucleus in and growth of hygroscopic droplets, *Trans. Faraday Soc.*, 32, 1152–1161, doi:10.1039/TF9363201152, 1936.
- Kreidenweis, S. M., Petters, M. D., and DeMott, P. J.: Single-parameter estimates of aerosol water content, *Environ. Res. Lett.*, 3, 035002 doi:10.1088/1748-9326/3/3/035002, 2008.
- 20 Kuwata, M., Kondo, Y., Mochida, M., Takegawa, N., and Kawamura, K.: Dependence of CCN activity of less volatile particles on the amount of coating observed in Tokyo, *J. Geophys. Res.*, 112, D11207, doi:10.1029/2006JD007758, 2007.
- Lance, S., Medina, J., Smith, J., and Nenes, A.: Mapping the operation of the DMT
25 continuous flow CCN counter, *Aerosol Sci. Technol.*, 40, 242–254, 2006.

- Lathem, T.L., and Nenes, A.: Water vapor depletion in the DMT Continuous Flow
CCN Chamber: effects on supersaturation and droplet growth, *Aeros.Sci.Tech.*, **45**,
604–615, doi:10.1080/02786826.2010.551146, 2011.
- Lathem, T. L., Beyersdorf, A. J., Thornhill, K. L., Winstead, E. L., Cubison, M. J.,
5 Hecobian, A., Jimenez, J. L., Weber, R. J., Anderson, B. E., and Nenes, A.: Analysis
of CCN activity of Arctic aerosol and Canadian biomass burning during summer
2008, *Atmos. Chem. Phys.*, **13**, 2735-2756, doi:10.5194/acp-13-2735-2013, 2013.
- Lau, K. M., Ramahathan, V., Wu, G., Li, Z., Tsay, S. C., Hsu, C., Sikka, R., Holben,
B., Lu, D., Tartari, G., Chin, M., Koudelova, P., Chen, H., Ma, Y., Huang, J.,
10 Taniguchi, K., and Zhang, R.: The joint aerosol monsoon experiment: A new
challenge for monsoon climate research, *Bull. Am. Meteorol. Soc.*, **89**, 369–383,
doi:10.1175/BAMS-89-3-369, 2008.
- Lee, S. H., Murphy, D. M., Thomson, D. S., and Middlebrook, A. M.: Nitrate and
oxidized organic ions in single particle mass spectra during the 1999 Atlanta
15 Supersite Project, *J. Geophys. Res.*, **108**, 8417, doi:10.1029/2001JD001455, 2003.
- Lee, Y. S., Collins, D. R., Li, R. J., Bowman, K. P., and Feingold, G.: Expected
impact of an aged biomass burning aerosol on cloud condensation nuclei and cloud
droplet concentrations, *J. Geophys. Res.*, **111**, D22204, doi:10.1029/2005JD006464,
2006.
- 20 Leng, C., Cheng, T., Chen, J., Zhang, R., Tao, J., Huang, G., Zha, S., Zhang, M., Fang,
W., Li, X., Li, L.: Measurements of surface cloud condensation nuclei and aerosol
activity in downtown Shanghai. *Atmos. Environ.*, **69**, 354-361, 2013.
- Liu, J., Zheng, Y., Li, Z., and Cribb, M.: Analysis of cloud condensation nuclei
properties at a polluted site in southeastern China during the AMF - China
25 Campaign, *J. Geophys. Res.*, **116**, D00K35, doi:10.1029/2011JD016395, 2011.

- Li, Z., Chen, H., Cribb, M., Dickerson, R. E., Holben, B., Li, C., Lu, D., Luo, Y.,
Maring, H., Shi, G., Tsay, S.-C., Wang, P., Wang, Y., Xia, X., Zheng, Y., Yuan, T.,
and Zhao, F.: Preface to special section on East Asian Studies of Tropospheric
Aerosols: An International Regional Experiment (EASTAIRE), *J. Geophys. Res.*,
5 112, D22S00, doi:10.1029/2007JD008853, 2007a.
- Li, Z., Xia, X., Cribb, M., Mi, W., Holben, B., Wang, P., Chen, H., Tsay, S.-C., Eck, T.
F., Zhao, F., Dutton, E. G., and Dickerson, R. E.: Aerosol optical properties and
their radiative effects in northern China, *J. Geophys. Res.*, 112, D22S01,
doi:10.1029/2006JD007382, 2007b.
- 10 Li, Z., Li, C., Chen, H., Tsay, S.-C., Holben, B., Huang, J., Li, B., Maring, H., Qian,
Y., Shi, G., Xia, X., Yin, Y., Zheng, Y., and Zhuang, G.: East Asian Studies of
Tropospheric Aerosols and Impact on Regional Climate (EAST - AIRC): An
overview, *J. Geophys. Res.*, 116, D00K34, doi:10.1029/2010JD015257, 2011.
- Liu, J., Zheng, Y., Li, Z., and Cribb, M.: Analysis of cloud condensation nuclei
15 properties at a polluted site in southeastern China during the AMF - China
Campaign, *J. Geophys. Res.*, 116, D00K35, doi:10.1029/2011JD016395, 2011.
- Ma, Y., Brooks, S. D., Vidaurre, G., Khalizov, A. F., Wang, L.: Rapid modification of
cloud-nucleating ability of aerosols by biogenic emissions, *Geophys. Res. Lett.* 40,
6293-6297, doi: 10.1002/2013GL057895, 2013.
- 20 Mei, F., Setyan, A., Zhang, Q., and Wang, J.: CCN activity of organic aerosols
observed downwind of urban emissions during CARES, *Atmos. Chem. Phys.*, 13,
12155–12169, doi:10.5194/acp-13-12155-2013, 2013.
- Mikhailov, E., Vlasenko, S., Martin, S. T., Koop, T., and Pöschl, U.: Amorphous
and crystalline aerosol particles interacting with water vapor: conceptual
25 framework and experimental evidence for restructuring, phase transitions and

kinetic limitations, Atmos. Chem. Phys., 9, 9491–9522,
doi:10.5194/acp-9-9491-2009, 2009.

Mircea, M., Facchini, M. C., Decesari, S., Cavalli, F., Emblico, L., Fuzzi, S., Vestin,
A., Rissler, J., Swietlicki, E., Frank, G., Andreae, M. O., Maenhaut, W., Rudich, Y.,
5 and Artaxo, P.: Importance of the organic aerosol fraction for modeling aerosol
hygroscopic growth and activation: a case study in the Amazon Basin, Atmos.
Chem. Phys., 5, 3111–3126, 2005, <http://www.atmos-chem-phys.net/5/3111/2005/>.

Niedermeier, D., Wex, H., Voigtländer, J., Stratmann, F., Brüggemann, E., Kiselev, A.,
Henk, H., and Heintzenberg, J.: LACIS-measurements and parameterization of
10 sea-salt particle hygroscopic growth and activation, Atmos. Chem. Phys., 8,
579–590, doi:10.5194/acp-8-579-2008, 2008.

Ng, N. L., Herndon, S. C., Trimborn, A., Canagaratna, M. R., Croteau, P. L., Onasch,
T. B., Sueper, D., Worsnop, D. R., Zhang, Q., Sun, Y. L., and Jayne, J. T.: An
Aerosol Chemical Speciation Monitor (ACSM) for Routine Monitoring of the
15 Composition and Mass Concentrations of Ambient Aerosol, Aerosol Sci. Tech., 45,
770–784, 2011.

Padr^o L. T., Tkacik, D., Lathem, T. L., Hennigan, C. J., Sullivan, A. P., Weber, R. J.,
Huey, L. G., and Nenes, A.: Investigation of cloud condensation nuclei properties
and droplet growth kinetics of the water-soluble aerosol fraction in Mexico City, J.
20 Geophys. Res., 115, D09204, doi:10.1029/2009JD013195, 2010.

Paramonov, M., Aalto, P. P., Asmi, A., Prisle, N., Kerminen, V.-M., Kulmala, M., and
Pet^ä T.: The analysis of size-segregated cloud condensation nuclei counter
(CCNC) data and its implications for aerosol-cloud interactions, Atmos. Chem.
Phys. Discuss., 13, 9681–9731, doi:10.5194/acpd-13-9681-2013, 2013.

- Petters, M. D., and Kreidenweis, S. M.: A single parameter representation of hygroscopic growth and cloud condensation nucleus activity, *Atmos. Chem. Phys.*, 7, 1961–1971, doi:10.5194/acp-7-1961-2007, 2007.
- Petters, M. D., Carrico, C. M., Kreidenweis, S. M., Prenni, A. J., DeMott, P. J.,
5 Collett, J. L., and Moosmüller, H.: Cloud condensation nucleation activity of biomass burning aerosol, *J. Geophys. Res.*, 114, D22205, doi:10.1029/2009JD012353, 2009.
- Quinn, P. K., Bates, T. S., Coffman, D. J., and Covert, D. S.: Influence of particle size and chemistry on the cloud nucleating properties of aerosols, *Atmos. Chem. Phys.*,
10 8, 1029–1042, 2008, <http://www.atmos-chem-phys.net/8/1029/2008/>.
- Raymond, T. M., and Pandis, S. N.: Cloud activation of single component organic aerosol particles, *J. Geophys. Res.*, 107, 4787, doi:10.1029/2002JD002159, 2002.
- Rissler, J., Swietlicki, E., Zhou, J., Roberts, G., Andreae, M. O., Gatti, L. V., and
15 Artaxo, P.: Physical properties of the submicrometer aerosol over the Amazon rain forest during the wet to dry season transition – comparison of modeled and measured CCN concentrations, *Atmos. Chem. Phys.*, 4, 2119–2143, <http://www.atmos-chem-phys.net/4/2119/2004/>, 2004.
- Roberts, G. C., Artaxo, P., Zhou, J. C., Swietlicki, E., and Andreae, M. O.: Sensitivity of CCN spectra on chemical and physical properties of aerosol: A case study from
20 the Amazon Basin, *J. Geophys. Res.*, 107, 8070, doi:10.1029/2001JD000583, 2002.
- Rose, D., Gunthe, S. S., Mikhailov, E., Frank, G. P., Dusek, U., Andreae, M. O., and Poschl, U.: Calibration and measurement uncertainties of a continuous-flow cloud condensation nuclei counter (DMT-CCNC): CCN activation of ammonium sulfate and sodium chloride aerosol particles in theory and experiment, *Atmos. Chem.*
25 *Phys.*, 8, 1153–1179, 2008, <http://www.atmos-chem-phys.net/8/1153/2008/>.

- Rose, D., Nowak, A., Achtert, P., Wiedensohler, A., Hu, M., Shao, M., Zhang, Y.,
Andreae, M. O., and Pöschl, U.: Cloud condensation nuclei in polluted air and
biomass burning smoke near the mega-city Guangzhou, China – Part 1:
Size-resolved measurements and implications for the modeling of aerosol particle
5 hygroscopicity and CCN activity, *Atmos. Chem. Phys.*, 10, 3365–3383,
doi:10.5194/acp-10-3365-2010, 2010.
- Rose, D., Gunthe, S. S., Su, H., Garland, R. M., Yang, H., Berghof, M., Cheng, Y. F.,
Wehner, B., Achtert, P., Nowak, A., Wiedensohler, A., Takegawa, N., Kondo, Y.,
Hu, M., Zhang, Y., Andreae, M. O., and Pöschl, U.: Cloud condensation nuclei in
10 polluted air and biomass burning smoke near the mega-city Guangzhou, China –
Part 2: Size-resolved aerosol chemical composition, diurnal cycles, and externally
mixed weakly CCN-active soot particles, *Atmos. Chem. Phys.*, 11, 2817–2836,
doi:10.5194/acp-11-2817-2011, 2011.
- Rosenfeld, D., Dai, J., Yu, X., Yao, Z., Xu, X., Yang, X., and Du, C.: Inverse
15 relations between amounts of air pollution and orographic precipitation, *Science*,
315(5817), 1396–1398, doi:10.1126/science.1137949, 2007.
- Salcedo, D., Onasch, T. B., Dzepina, K., Canagaratna, M. R., Zhang, Q., Huffman, J.
A., DeCarlo, P. F., Jayne, J. T., Mortimer, P., Worsnop, D. R., Kolb, C. E., Johnson,
K. S., Zuberi, B., Marr, L. C., Volkamer, R., Molina, L. T., Molina, M. J., Cardenas,
20 B., Bernabe, R. M., Marquez, C., Gaffney, J. S., Marley, N. A., Laskin, A.,
Shutthanandan, V., Xie, Y., Brune, W., Leshner, R., Shirley, T., and Jimenez, J. L.:
Characterization of ambient aerosols in Mexico City during the MCMA-2003
campaign with Aerosol Mass Spectrometry: results from the CENICA Supersite,
Atmos. Chem. Phys., 6, 925–946, 2006.
- 25 Sotiropoulou, R. E. P., Nenes, A., Adams, P. J., and Seinfeld, J. H.: Cloud

- condensation nuclei prediction error from application of Köhler theory: Importance for the aerosol indirect effect, *J. Geophys. Res.*, 112, D12202, doi:10.1029/2006JD007834, 2007.
- Streets, D. G., Yu, C., Wu, Y., Chin, M., Zhao, Z., Hayasaka, T., and Shi, G.: Aerosol trends over China, 1980–2000, *Atmos. Res.*, 88, 174–182, doi:10.1016/j.atmosres.2007.10.016, 2008.
- Stroud, C. A., Nenes, A., Jimenez, J. L., DeCarlo, P., Huffman, J. A., Bruintjes, R., Nemitz, E., Delia, A. E., Toohey, D. W., Guenther, A. B., and Nandi, S.: Cloud Activating Properties of Aerosol Observed during CELTIC, *J. Atmos. Sci.*, 64, 441–459, 2007.
- Sun, Y., Wang, Z., Dong, H., Yang, T., Li, J., Pan, X., Chen, P., and Jayne, J. T.: Characterization of summer organic and inorganic aerosols in Beijing, China with an Aerosol Chemical Speciation Monitor, *Atmos. Environ.*, 51, 250–259, doi:10.1016/j.atmosenv.2012.01.013, 2012.
- Takegawa, N., Miyakawa, T., Kawamura, K., and Kondo, Y.: Contribution of selected di-carboxylic and omega-oxocarboxylic acids in ambient aerosol to the m/z 44 signal of an aerodyne aerosol mass spectrometer, *Aerosol Sci. Technol.*, 41, 418–437, doi:10.1080/02786820701203215, 2007.
- Turpin, B. J., and Lim, H. J.: Species contributions to PM_{2.5} mass concentrations: Revisiting common assumptions for estimating organic mass, *Aerosol Sci. Tech.*, 35, 602–610, 2001.
- Twomey, S.: Pollution and planetary albedo, *Atmos. Environ.*, 8, 1251–1256, 1974.
- VanReken, T. M., Rissman, T. A., Roberts, G. C., Varutbangkul, V., Jonsson, H. H., Flagan, R. C., and Seinfeld, J. H.: Toward aerosol/cloud condensation nuclei (CCN) closure during CRYSTAL-FACE, *J. Geophys. Res.*, 108, 4633,

doi:10.1029/2003JD003582, 2003.

VanReken, T. M., Ng, N. L., Flagan, R. C., and Seinfeld, J. H.: Cloud condensation nucleus activation properties of biogenic secondary organic aerosol, *J. Geophys. Res.*, 110, D07206, doi:10.1029/2004JD005465, 2005.

5 Varutbangkul, V., Brechtel, F. J., Bahreini, R., Ng, N. L., Keywood, M. D., Kroll, J. H., Flagan, R. C., Seinfeld, J. H., Lee, A., and Goldstein, A. H.: Hygroscopicity of secondary organic aerosols formed by oxidation of cycloalkenes, monoterpenes, sesquiterpenes, and related compounds, *Atmos. Chem. Phys.*, 6, 2367–2388, 2006.

Whitby, K., T.: The physical characteristics of sulfur aerosols. *Atmos. Environ.*, 12,
10 135-159, 1967, Online publication date: 1-Jan-1978, 1978.

Xia, X., Li, Z., Holben, B., Wang, P., Eck, T., Chen, H., Cribb, M., and Zhao, Y.: Aerosol optical properties and radiative effects in the Yangtze Delta region of China, *J. Geophys. Res.*, 112, D22S12, doi:10.1029/2007JD008859, 2007.

Xin, J., Wang, Y., Li, Z., Wang, P., Hao, W., Nordgren, B. L., Wang, S., Liu, G.,
15 Wang, L., Wen, T., Sun, Y., Hu, B.: AOD and Angstrom exponent of aerosols observed by the Chinese Sun Hazemeter Network from August 2004 to September 2005, *J. Geophys. Res.*, 112, D05203, doi:10.1029/2006JD007075, 2007.

Xu, Q.: Abrupt change of the mid - summer climate in central east China by the influence of atmospheric pollution, *Atmos. Environ.*, 35, 5029–5040,
20 doi:10.1016/S1352-2310(01)00315-6, 2001.

Yue, D. L., Hu, M., Zhang, R. J., Wu, Z. J., Su, H., Wang, Z. B., Peng, J. F., He, L. Y., Huang, X. F., Gong, Y. G., and Wiedensohler, A.: Potential contribution of new particle formation to cloud condensation nuclei in Beijing, *Atmos. Environ.*, 45, 6070-6077, 2011.

25 Yum, S. S., Roberts, G., Kim, J. H., Song, K., and Kim, D.: Submicron aerosol size

distributions and cloud condensation nuclei concentrations measured at Gosan, Korea, during the Atmospheric Brown Clouds–East Asian Regional Experiment 2005, *J. Geophys. Res.*, 112, D22S32, doi:10.1029/2006JD008212, 2007.

5 Zhang, Q., Meng, J., Quan, J., Gao, Y., Zhao, D., Chen, P., and He, H.: Impact of aerosol composition on cloud condensation nuclei activity, *Atmos. Chem. Phys.*, 12, 3783–3790, doi:10.5194/acp-12-3783-2012, 2012.

Zhang, Q., Stanier, C. O., Canagaratna, M. C., Jayne, J. T., Worsnop, D. R., Pandis, S. N., and Jimenez, J. L.: Insights into the Chemistry of New Particle Formation and Growth Events in Pittsburgh Based on Aerosol Mass Spectrometry, *Environ. Sci. Technol.*, 38, 4797–4809, 2004.

10

Zhang, R., Khalizov, A. F., Pagels, J., Zhang, D., Xue, H., and McMurry, P. H.: Variability in morphology, hygroscopic and optical properties of soot aerosols during internal mixing in the atmosphere, *Proc. Natl. Acad. Sci. USA* 105, 10291–10296, 2008.

15

20

25

Tables and Figures

Table 1. Parameters describing the CCN efficiency spectra and hygroscopicity for polluted (*_POL) and background (*_BG) cases: the activation diameter (D_a), the maximum activated fraction (MAF), the CDF standard deviation (σ), the heterogeneity parameter (σ/D_a), and the hygroscopicity parameter (κ_a). Values shown are arithmetic mean values with one standard deviation averaged over the entire measurement period.

SS	D_{a_POL}	MAF_POL	σ_POL	σ/D_{a_POL}	κ_{a_POL}	D_{a_BG}	MAF_BG	σ_BG	σ/D_{a_BG}	κ_{a_BG}
0.08%	190.43±6.11	0.98±0.01	33.34±4.49	0.17±0.02	0.32±0.03	178.68±4.22	0.98±0.01	32.73±2.07	0.18±0.01	0.38±0.02
0.11%	161.80±15.10	0.98±0.01	38.61±7.62	0.22±0.03	0.26±0.05	151.03±2.90	0.97±0.01	28.56±1.97	0.19±0.01	0.33±0.02
0.23%	94.05±8.47	0.96±0.01	27.87±6.30	0.26±0.04	0.31±0.05	91.75±2.48	0.96±0.00	18.81±1.53	0.20±0.01	0.34±0.02
0.42%	63.33±3.65	0.94±0.01	18.02±2.84	0.26±0.03	0.30±0.04	64.06±1.24	0.95±0.00	16.21±0.81	0.25±0.01	0.29±0.01
0.80%	44.78±2.51	0.94±0.01	14.08±0.98	0.29±0.01	0.24±0.03	45.67±1.29	0.95±0.01	13.82±1.17	0.30±0.02	0.22±0.02

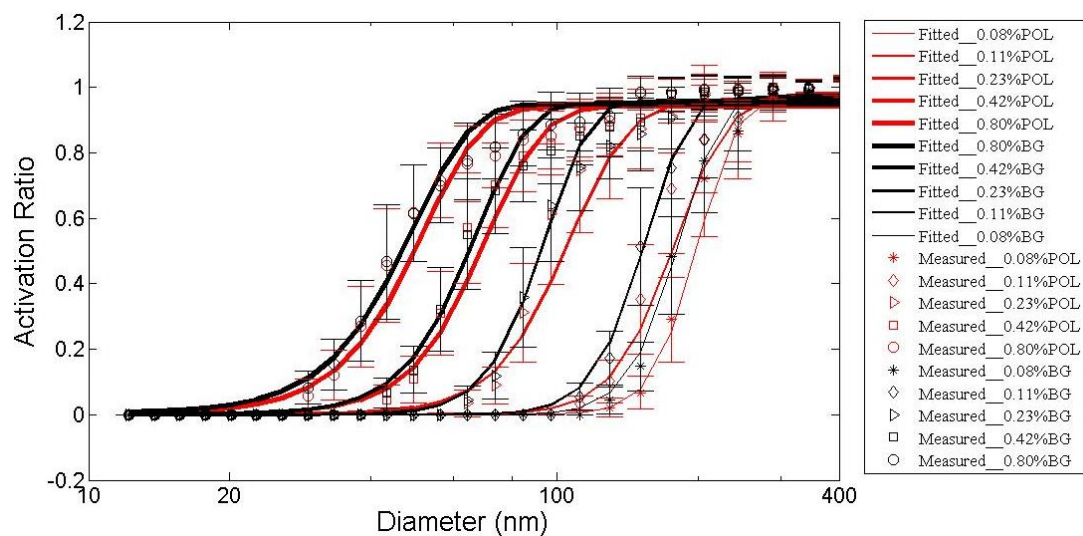


Fig. 1. Averaged measured and fitted CCN efficiency spectra from the 3-parameter CDF fit at SS = 0.08%, 0.11%, 0.23%, 0.42%, and 0.80% under polluted (POL) and background (BG) conditions during the size-resolved CCN measurement period.

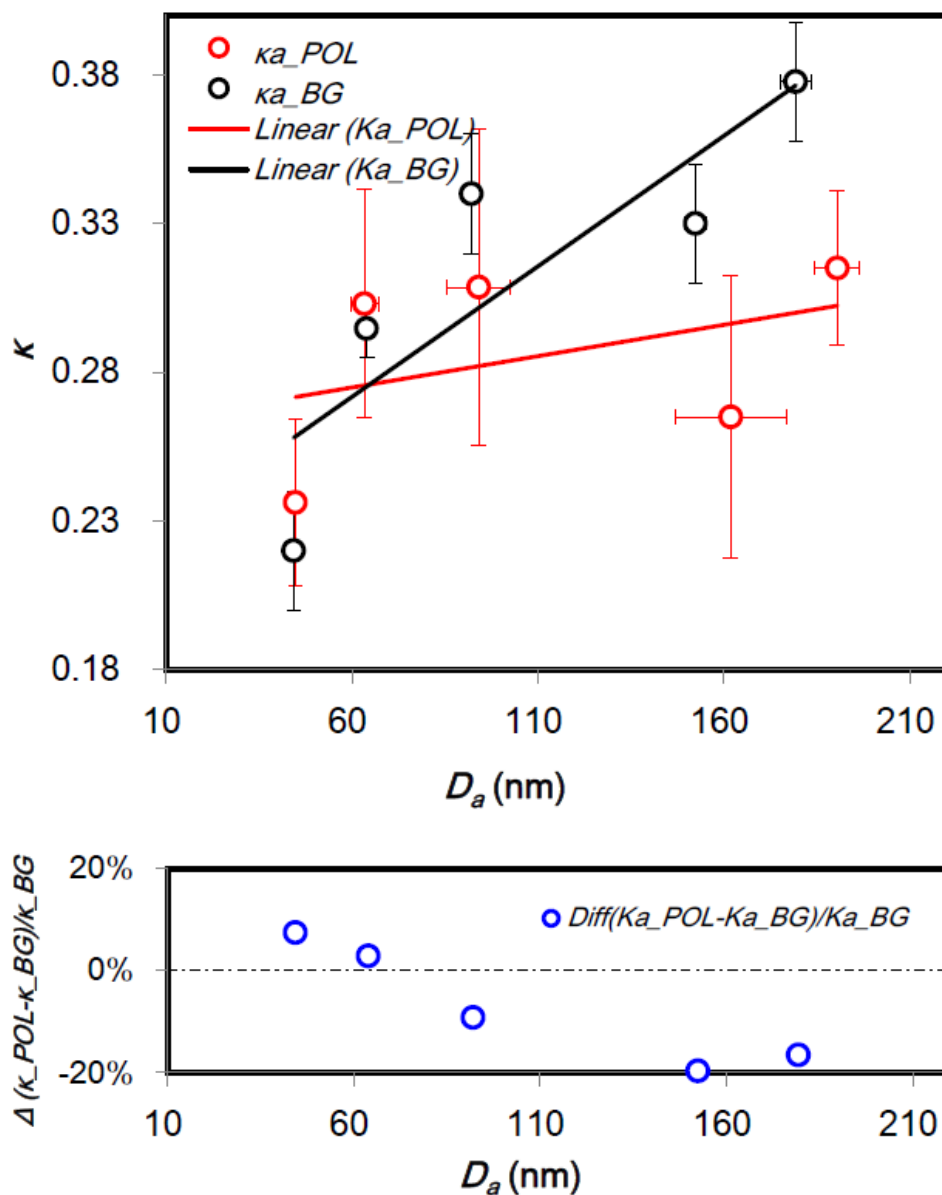


Fig. 2. Top: Derived hygroscopicity parameter, κ_a , as a function of particle diameter, D_a , under polluted (POL) and background (BG) conditions. **Bottom:** Percent change in κ_a due to pollution as a function of D_a . Error bars represent one standard deviation calculated over the entire measurement period.

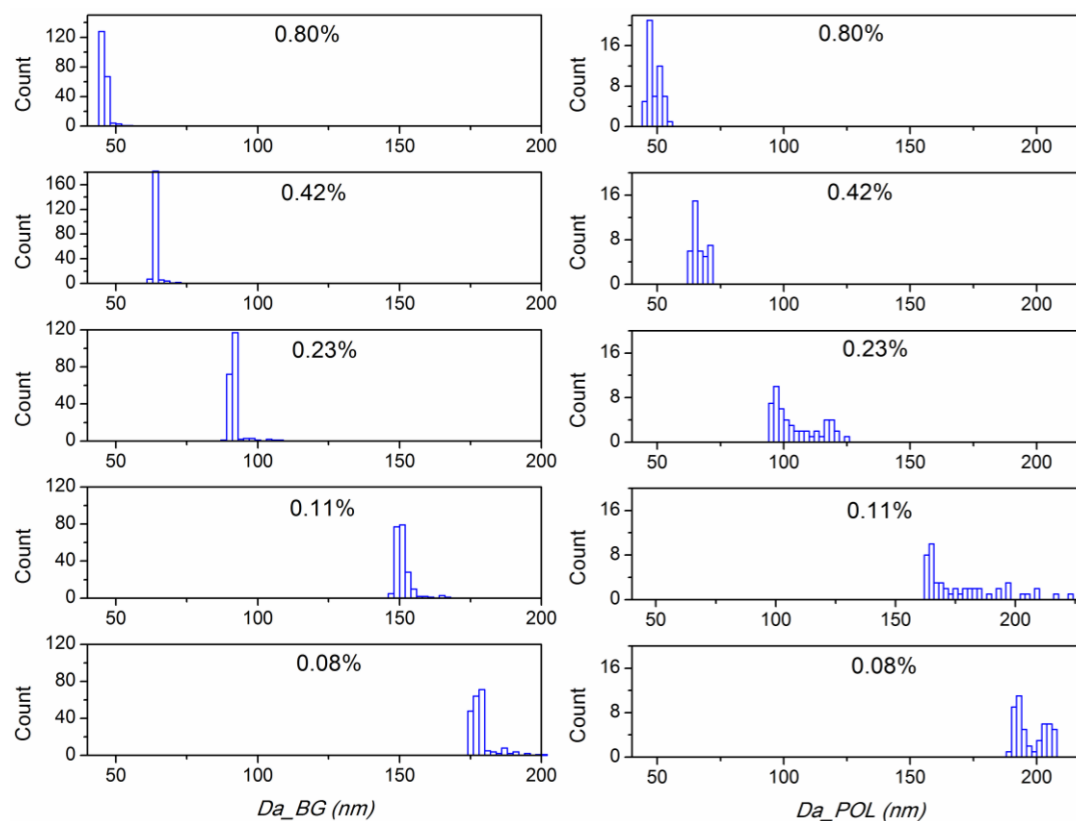


Fig. 3. Probability distribution functions of D_a under background and polluted conditions at five SS levels (0.08-0.80%) during the size-resolved CCN measurement period.

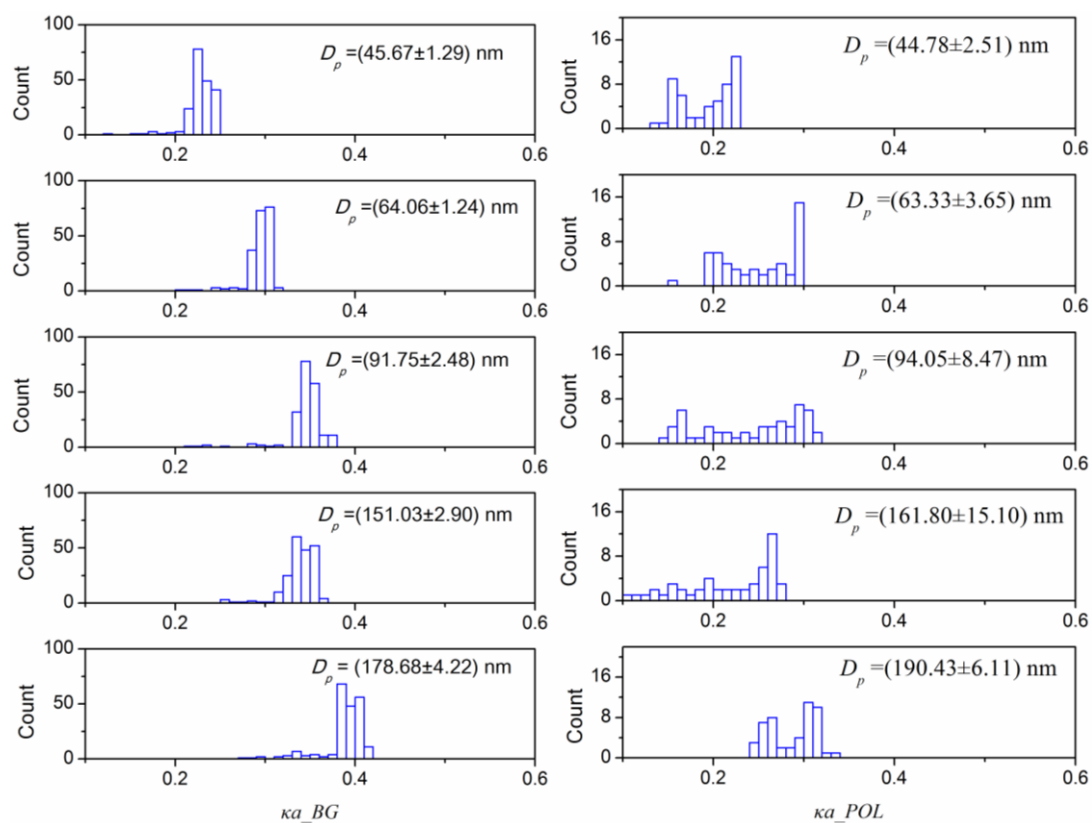


Fig. 4. Probability distribution functions of κ_a under background (left panels) and polluted (right panels) conditions for different particle size ranges during the size-resolved CCN measurement period.

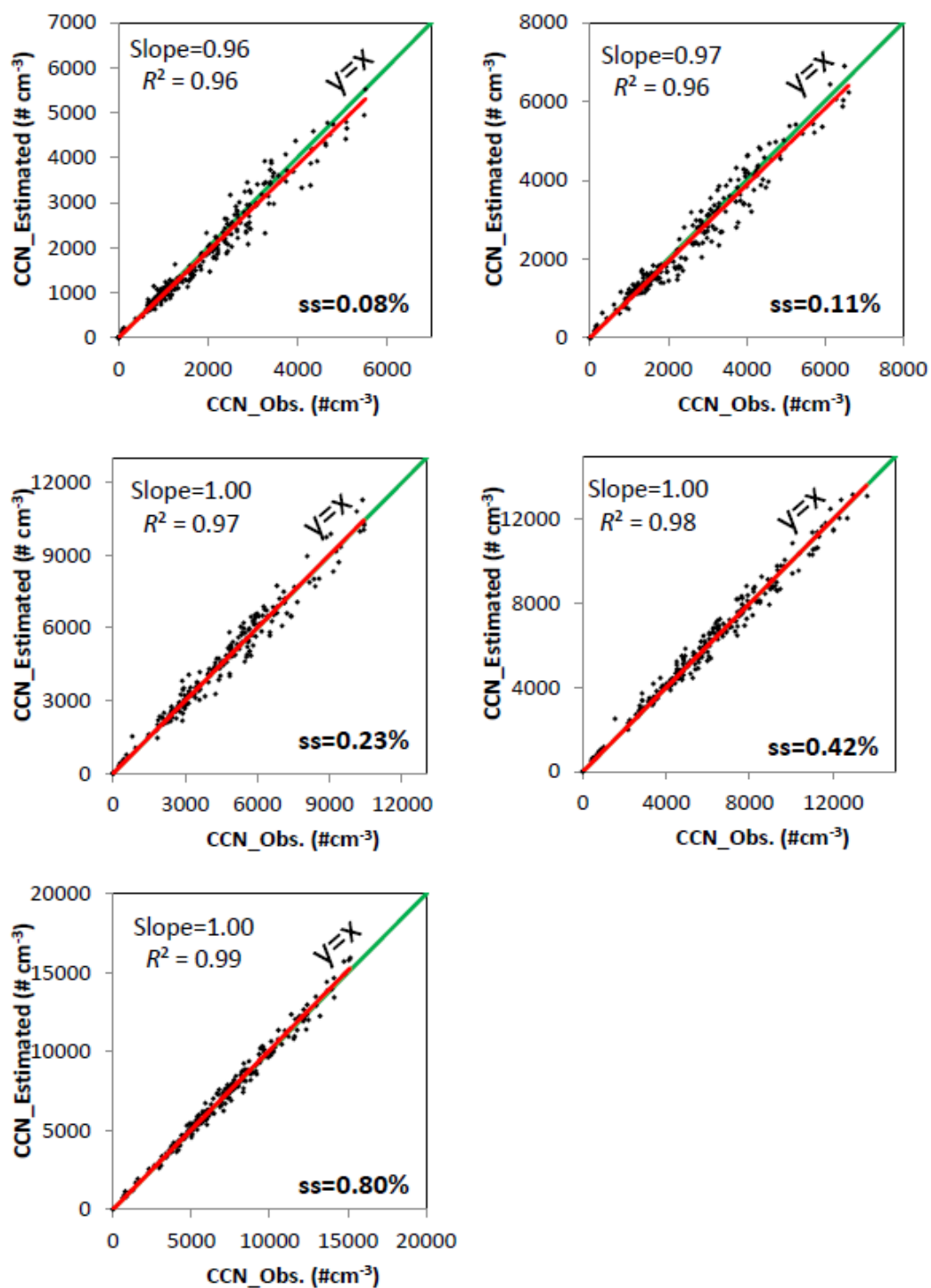


Fig. 5. Estimated N_{CCN} as a function of observed N_{CCN} at different SS levels in the parallel observation (PO) closure test. The green solid line is the 1:1 line.

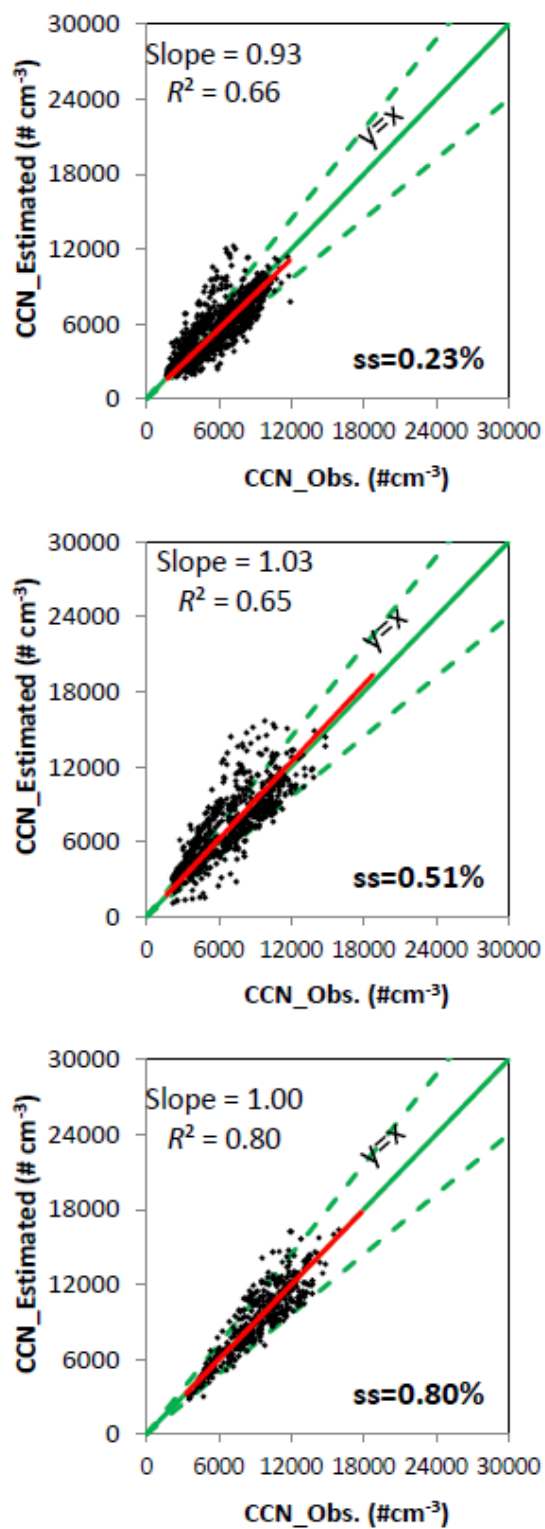


Fig. 6. As in Figure 5, but for the non-parallel observation (NPO) closure test. The dashed green lines indicate the boundaries representing $\pm 30\%$ deviations of $N_{\text{CCN-estimated}}$ from $N_{\text{CCN-observed}}$.

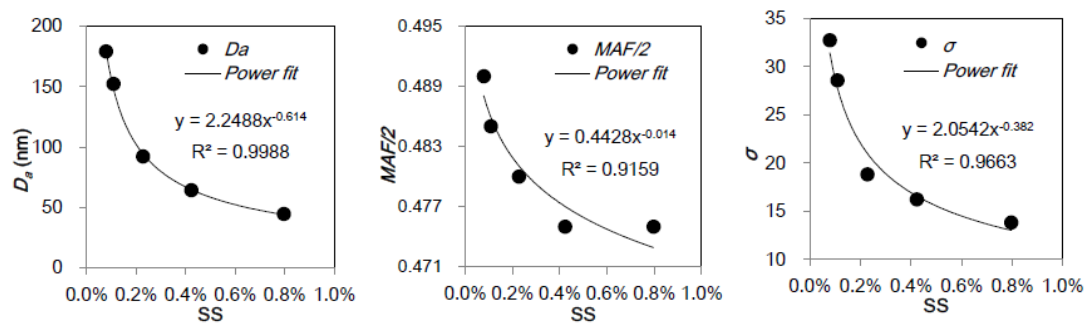


Fig. 7. D_a , MAF , and σ as a function of SS .

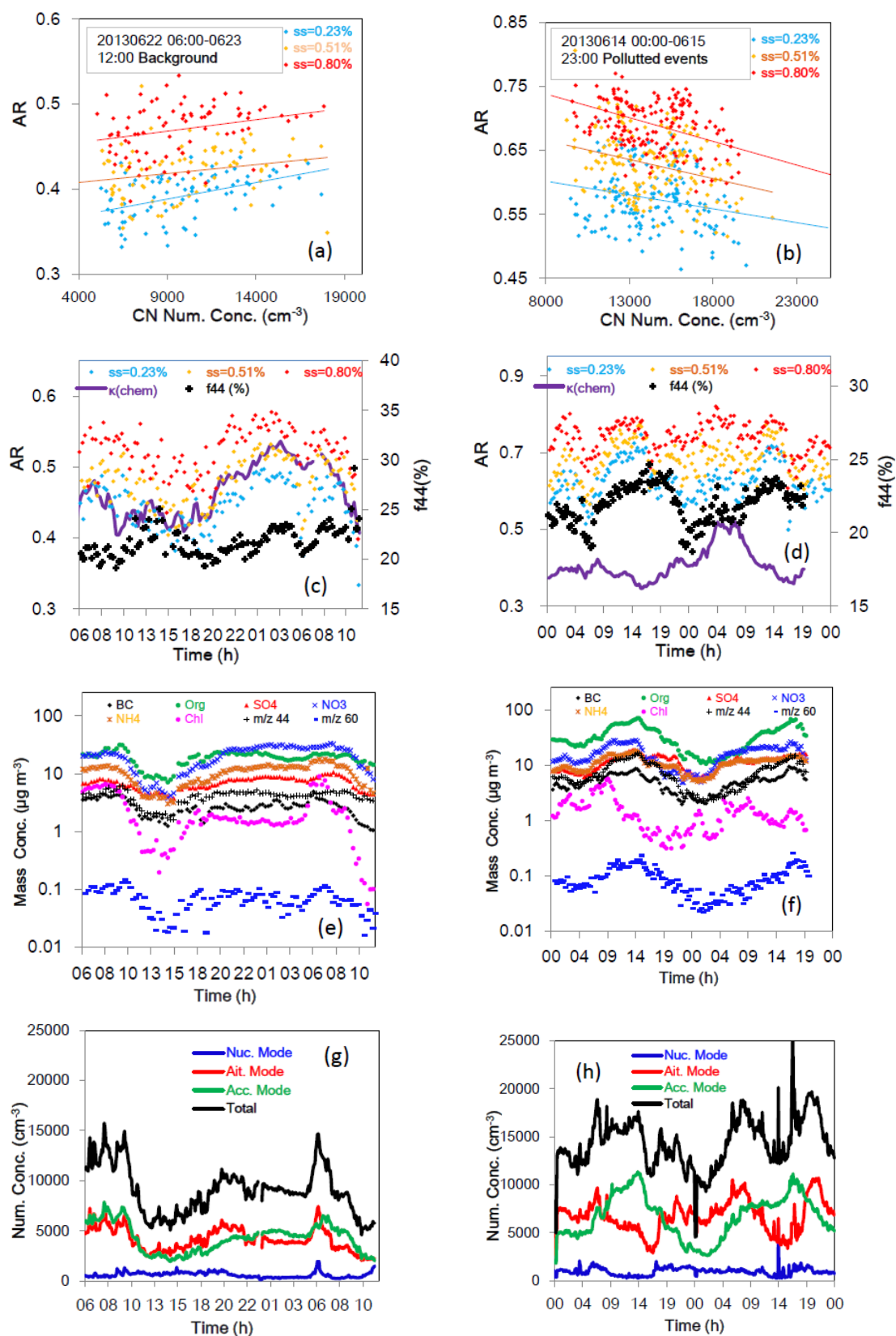


Fig. 8. Measurements made under background conditions (22-23 June 2013, N_{CN} of $< 15000 \text{ cm}^{-3}$) and polluted conditions (14-15 June 2013, N_{CN} of $> 15000 \text{ cm}^{-3}$). Bulk CCN activation ratios at SS = 0.2%, 0.5%, and 0.8% as a function of N_{CN} under

background and polluted conditions are shown in Fig. 8a and Fig. 8b, respectively. Diurnal variations in AR, derived from κ_{chem} and the fraction of total organic mass signal at f_{44} , under background and polluted conditions are shown in Fig. 8c and Fig. 8d, respectively. Mass concentrations of black carbon (BC), organics, nitrate (NO_3^-), ammonium (NH_4^+), sulfate (SO_4^{2-}), chloride (Cl^-) ions, etc., under background and polluted conditions are shown in Fig. 8e and Fig. 8f, respectively. N_{CN} for nucleation (10-30 nm), Aitken (30-130 nm), and accumulation modes (130-700 nm) under background and polluted conditions are shown in Fig. 8g and Fig. 8h, respectively.

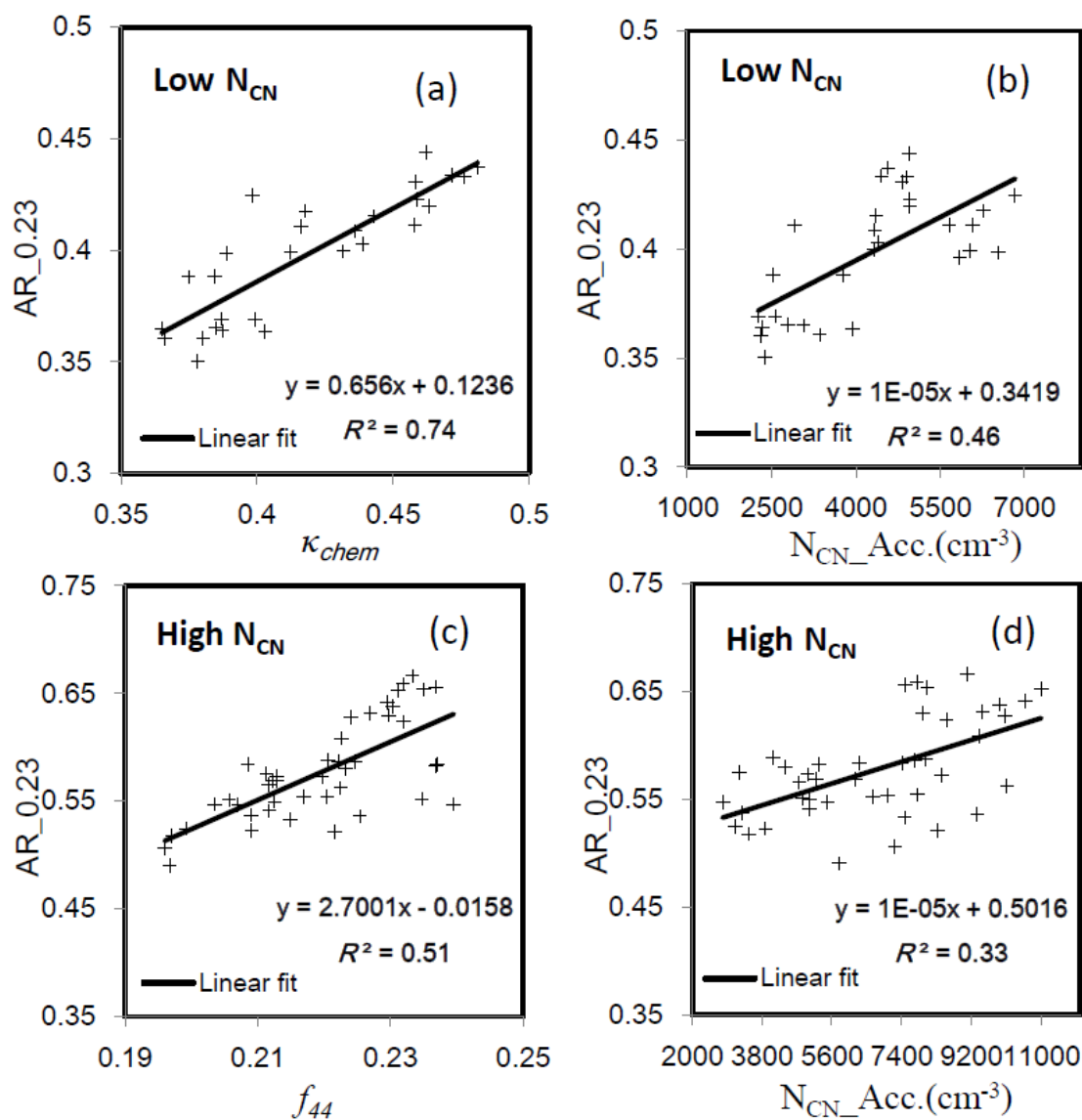


Fig. 9. AR measured at SS = 0.23% as a function of (a) κ_{chem} under background conditions, (b) accumulation mode N_{CN} under background conditions, (c) f_{44} under polluted conditions, and (d) accumulation mode N_{CN} under polluted conditions. The accumulation mode size range is 130-700 nm in this study.

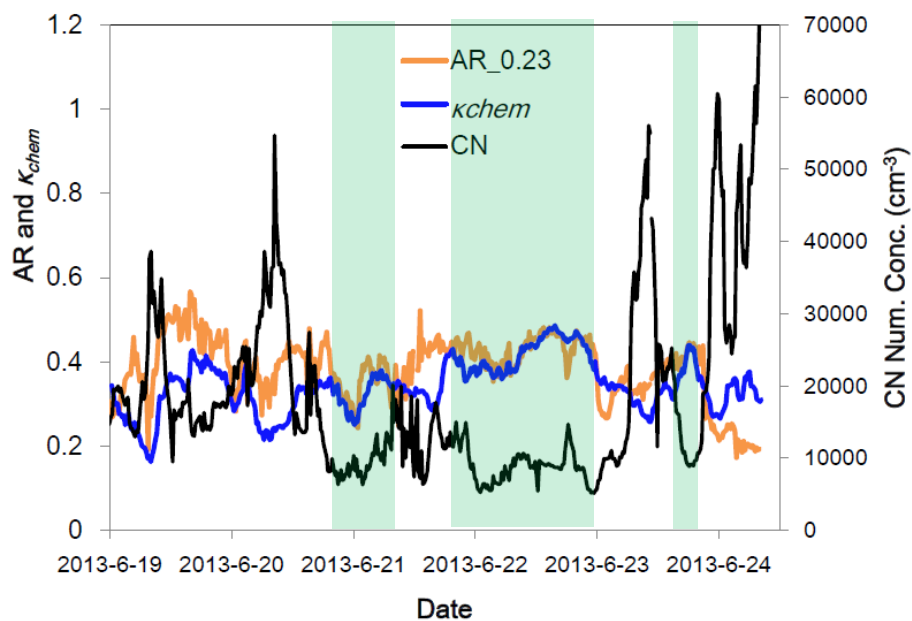


Fig. 10. Time series of bulk AR at SS = 0.23%, derived κ_{chem} , and N_{CN} from 19-24 June 2013. Green shaded areas highlight periods when there was a high correlations between bulk AR and κ_{chem} .